INL/CON-07-13435
PREPRINT

First Principle Quantum Description of the Energetics Associated with $LaBr_3$, $LaCl_3$, and Ce Doped Scintillators

NSS-MIC-07

Michael E. McIlwain
Da Gao
Nick Thompson

December 2007

The INL is a
U.S. Department of Energy
National Laboratory
operated by
Battelle Energy Alliance

First Principle Quantum Description of the Energetics Associated with $LaBr_3$, $LaCl_3$, and Ce Doped Scintillators

Michael E. McIlwain, Da Gao, and Nick Thompson

Abstract-Considerable interest is given to the excellent scintillation properties of cerium doped lanthanum chloride ($LaCl_3$) and lanthanum bromide ($LaBr_3$). The scintillation efficiencies are much greater than other materials, even those containing cerium. This high efficiency is attributed to the high mobility of electrons and holes, unique placement of the cerium 5d states within the band gap, and energy of the band gap. To better understand the scintillation process and better define the nature of the Self Trapped Exciton (STE) within these unique scintillation materials, density functional theory (DFT), and Ab-*inito* (HF-MP2) calculations are reported. DFT calculations have yielded a qualitative description of the orbital composition and energy distribution of the band structure in the crystalline material. MP2 and single configuration interaction calculations have provided quantitative values for the band gap and provided energies for the possible range of excited states created following hole and electron creation. Based on this theoretical treatment, one possible description of the STE is the combination of V_k center (Br_2^{-1}) and $LaBr^{+1}$ species that recombine to form a distorted geometry $LaBr_3^*$ (triplet state). Depending on the distance between the LaBr and Br_2, the STE emission band can be reproduced.

I. Introduction

Over the last seven to eight years, considerable attention was given to the characterization of the photophysical properties of cerium doped lanthanum halides (Cl, Br) that were shown to be outstanding scintillators.

Manuscript submitted on May 11, 2007. This work was supported by the U. S. Department of Energy, Office of Biological and Environmental Research, Environmental Research Science Program under Contract No. DE AC07-05ID141517.

M. E. McIlwain, corresponding author, is with the Idaho National Laboratory, Idaho Falls, ID 83415 USA (telephone 208-526-8130, Michael.McIlwain@inl.gov)

D. Gao is with Washington State University, Pullman WA 99164 USA (telephone 208-526-3691, Da.Gao@inl.gov)

N. Thompson is with the Idaho National Laboratory, Idaho Falls, ID 83415 USA (telephone 208-526-0693, Nick.Thompson@inl.gov).

Spectroscopic measurements were performed to characterize the scintillation properties of both cerium doped lanthanum chloride and bromide [1]-[3]. These studies revealed that the photophysics of cerium scintillation was dependent on cerium concentration, halogen, and crystal temperature.

The scintillation process in $LaBr_3$ was shown to be composed of two mechanisms [4]. A fast mechanism that occurs almost immediately due to trapping of free holes and electrons by cerium leads to a temperature independent scintillation process. A thermally activated process involved hole and electron trapping by a Self Trapped Exciton (STE) followed by subsequent energy transfer to cerium. This second process was shown to be highly dependent on cerium concentration and decreased in importance as the crystal temperature was elevated above 100 K.

Theoretical treatments of the scintillation process using first principle *Ab-initio* methods were employed to characterize the nature of the STE in alkali halide scintillators, such as $NaI(Tl^+)$[5]-[9] and other wide band gap insulators[10],[11]. Based on these treatments, the electron and hole pair were represented by an electron placed in a Gaussian well located in a crystal defect and X_2^{-1}. The X_2^{-1} was also linked to the V_k defect. X_2^{-1} or hole mobility was shown to be due to vibration wavefunction overlap between adjacent X pairs [12].

Cluster coupled calculations were used to characterize the optical absorption energy of cerium in $LaBaF_5$:Ce crystals [13]. Band structure calculations were used to predict band gaps and location of the 4f levels of cerium in an oxide host of $LaAlO_2$ [14]. Hartree-Fock, Møller Plesset (HF-MP2) calculations were used to predict the vibrational frequencies of the trihalides [15]. Cluster calculation using a many electron approach was employed to predict the atomistic nature and spectroscopic properties of defects in wide band gap insulators [10].

In this paper, we have applied first principle quantum mechanical approaches to understand the

molecular nature and energetics associated with the electron and hole pair and the STE generated when ionizing radiation of energy greater than the band gap is absorbed by $LaBr_3$ and $LaCl_3$ and their Ce doped analogs. These approaches have been used to characterize the band structure of each crystal, characterize the molecular species that result from the electron and hole pair created in the ionization track, and investigate the recombination and transfers energy to cerium.

II. Computational Methodology

The objective of this study was to characterize the photophysics of scintillation and to understand the molecular species responsible for the transport of energy once the electron and hole pair were formed. To achieve this objective, a variety of computational approaches were needed. A qualitative description of the band gap and atomic orbital contribution to the band gap structure was needed for pure $LaBr_3$ and $LaCl_3$ and Ce doped crystal material and was obtained using a plane wave density functional theory (DFT) approach employed in the CASTEP [16]code. La, Br, and Cl were represented by ultra-soft pseudo potentials arranged in a muffin tin arrangement. The DFT calculations used the local density approximation and a ca-pz exchange correlation potential [17]. Since DFT is known to provide poor estimates of excited state energies, a quantitative description of the energy separation of the valence and conduction bands was obtained using an all-electron full-potential linearized augment plane wave code that employed a screened exchange local density approximation [18]. Calculation of the structure or ground state energies of molecular systems involving molecular configurations in the gas phase were obtained using either DFT or Hartree-Fock (HF) all electron calculations. To enhance the accuracy of the HF calculations, second order Møller-Plesset perturbation theory (MP2) [19] was applied. These calculations were performed using a Gaussian based approach implemented in several codes, such as NWCHEM [20] and QCHEM 3.0[21]. To obtain the excited singlet and triplet energies, both single excitation configuration interaction (xCIS) HF [22] and time dependent (TD) DFT calculation were performed. Pseudo potentials employed for La and Br were based on extended core potentials (ECPs) (CRENBL[23] and SBKJC [24])while an all electron self consistent double zeta basis set (aug-cc-pvdz[25]) was employed for Cl. DFT ground state calculations were performed using a numerical basis set approach employed by DMOL3[26],[27]. For DMOL3 calculations, all electron and DFT pseudopotentials approaches were used for La, Br, and Cl based calculations.

III. Results

Prior work has suggested that when ionizing radiation having energy greater than the band gap in a material is absorbed, and electrons are promoted from the valence band to the conduction band. This process creates holes (electron deficiencies) in the valence band. Prior theoretical results [7] have suggested that for alkali halide, wide band gap insulators, the hole can be represented by halide anion (X_2^-). This is also suggested by a recent paper [4] discussing STE energetics in LaX_3 scintillators[28]. Table 1 and Fig. 1 provide modeling results for pure $LaBr_3$ and $LaCl_3$ scintillators. The band gap energies given in Table 1 confirm prior modeling results that found that conventional DFT calculations under estimate the band gap while HF-MP2 calculations over estimate the energy of the gap [4]. DFT calculations that include screening potentials provided reasonable estimates of the band gap. Also included in Table 1 is a comparison of calculated and experimental values for the 4f-5d Ce energies in each crystal having a 5 weight percent Ce concentration. Fig. 1. displays the Density-of-States (DoS) representation for the pure crystal of $LaBr_3$. An orbital analysis of this representation is also provided and supports a conclusion that the valence band in the crystal is primarily composed of Br s and p orbitals. The conduction band is primarily composed of La d and f orbitals. In the crystal, La is surrounded by nine bromide ions. This subunit can be exactly modeled and the resulting orbital plots are shown in Fig. 2. The highest occupied molecular orbital (HOMO) (Fig. 2a) is composed of Br p orbitals and the lowest unoccupied molecular orbital (LUMO) (Fig. 2b) is composed of La d orbitals. We can use DoS information and orbital representations to develop a chemical explanation to describe the photo-events creating an electron and hole pair.

TABLE 1
CALCULATED AND EXPERIMENTAL BAND GAP ENERGIES (eV)

	DFT	SX-DFT	HF-MP2	EXP
$LaCl_3$	4.34	6.85	8.25	7.0+
$LaBr_3$	3.42	5.15	7.43	5.6+
LaI_3	0.3	2.48	6.92	3.3+
$LaCl_3$:Ce*	1.54			3.54
$LaBr_3$:Ce*	1.29			3.24

* Energy of the 4f to 5d Ce electronic transition

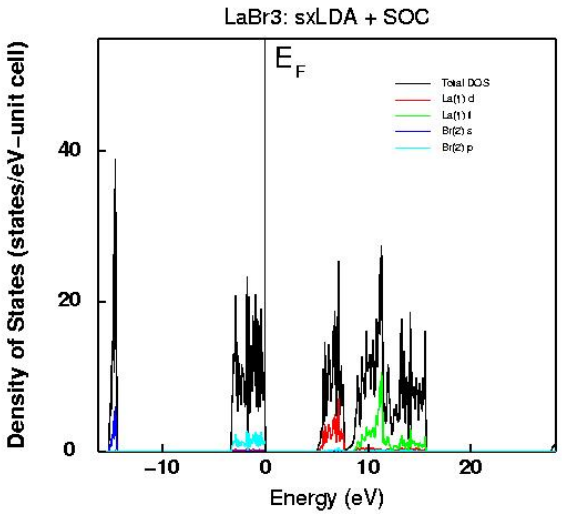

Fig. 1. DoS plot produced by FLAPW sx-LDA program for $LaBr_3$, conduction band begins at about 6.0 eV, green and red plots are La f and d orbitals respectively.

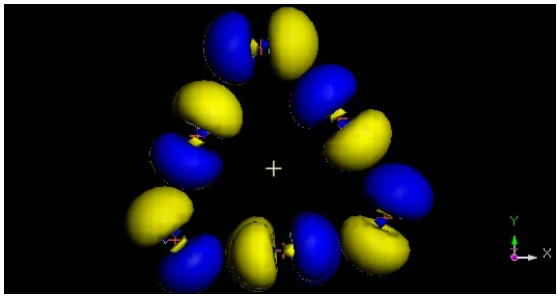

Fig. 2a. $LaBr_9$, DMOL3 plot of the highest occupied molecular orbital. La ion represented by yellow plus.

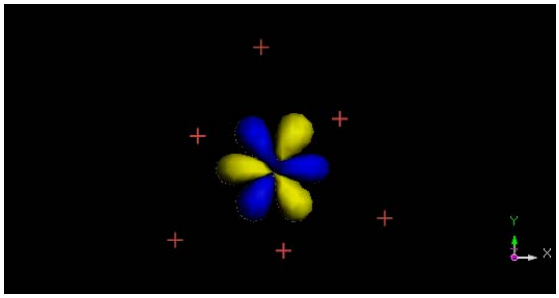

Fig. 2b. $LaBr_9$, Lowest unoccupied molecular orbital. Bromide ions represented by red pluses.

The electron deficiency is created in the bromine p orbitals and a reductive addition of an electron occurs to the La d orbitals.

This result suggests the following possible descriptions for the electron and hole in $LaBr_3$:

Hole Formation

$$Br^{-1} \rightarrow Br^{0} + e^{-} \quad (1)$$

$$Br^{-1} + Br^{0} \rightarrow Br_2^{-1} \quad (2)$$

Electron Trapping

$$La^{+3} + e^{-} \rightarrow La^{+2} \quad (3)$$

$$La^{+2} + Br^{-1} \rightarrow LaBr^{+} \quad (4)$$

STE Formation

$$LaBr^{+} + Br_2^{-1} \rightarrow LaBr_3^{*} \quad (5)$$

or

$$LaBr^{+} + Br_2^{-1} \rightarrow LaBr + Br_2^{*} \quad (6)$$

A similar set of reactions may also be developed for $LaCl_3$. For simplicity only LaBr will be discussed. Reaction (1) occurs as the photon is absorbed. The resulting electron is promoted from the valence band to the conduction band. Due to the confined geometry of the crystal, there is a high probability that an adjacent bromide ion will interact with the bromine atom to form the molecule. Reaction (2) was suggested by prior studies [11], and the resulting complex is called a V_k center. In a pure, perfect crystal, the electron in the conduction band is not bound to any particular La ion. However, in real crystals defects and lattice dislocations exist and the electron will ultimately be trapped by a La ion or in the case of Ce doped crystals by a Ce ion. This situation is quite different from the case of alkali halide scintillators where the electron is trapped by the defect. Reaction (3) results in the electron reducing a specific La ion. Reaction 4 is postulated due to the close proximity of numerous Br ions. Based on the thermodynamic data shown in Table 2, the $LaBr^{+}$ complex is not stable and will immediately proceed to either (5) or (6).

It should be noted that the proposed molecular species are not anticipated to exist in the locations represented by the equilibrium crystal position, but will depend on optimum molecular configurations and crystal temperature. DFT ground state calculations suggest the bond distances given in Table 2 may be representative of the molecular geometries. In addition, the binding energy of the molecule depends on the bond distance. These

differences are observed between the crystal bond length (0.3067 nm) and the optimum bond lengths.

The exact chemical nature of the $LaBr_3$ STE depends on which occurs, (5) or (6). Using the binding energy data given in Table 2, both reactions appear to be the favorable. However, Reaction (5) is much more energetic (671.5 kJ vs. 60.71 kJ) than (6).

TABLE 2
CALCULATED BOND LENGTHS AND BINDING ENERGIES

MOLECULE	BOND LENGTH (nm)	BINDING ENERGY (kJ)
Br_2	0.2330	-241.00
Br_2	0.2964	-112.98
Br_2^-	0.2964	-494.07
$LaBr^+$	0.2649	10.86
$LaBr^+$	0.3067	115.85
$LaBr^0$	0.3067	-431.57
$LaBr_3$	0.3067	-1219.8
$CeBr^+$	0.2622	-140.86
$CeCl^+$	0.2464	-200.32
$LaCl^+$	0.2493	-45.56
$LaCl_3$	0.2588	-1645.8
$LaCl_3$	0.3067	-1262.7
$CeCl_3$	0.2529	-1748.7
$CeCl_3$	0.3067	-1337.5
$CeBr_3$	0.2703	-1590.4
$CeBr_3$	0.3067	-1297.9

X-ray excited luminescence for pure $LaBr_3$ at 100K has two bands near 340 and 430 nm that are attributed to STE luminescence [3]. Similar bands are also observed for pure $LaCl_3$ [29]. xCIS-HF calculations were performed on various geometries of $LaBr_3$ and Br_2 to determine which molecule produced excited triplet state energies that compared with the observed experimental results. It should be noted that CIS-HF excited state energies are considered to be qualitative, since errors as large as 1 eV are reported [22]. However, the number of states and their approximate spacing are considered to be representative of those experimentally determined.

Using a diatomic bond distance for bromine of about 0.2460 nm, triplet transitions are predicted at 850, 450, and 370 nm. A singlet at 525 nm is also predicted, but the calculated oscillator (absorption and emission) strength is zero. The lowest energy triplet transition is always predicted and occurred between 1.15 μm and 800 nm.

In the case of $LaBr_3$, a distorted geometry shown in Fig. 3 is found to produce the experimental STE emission wavelengths. This distorted geometry can be characterized as LaBr and a pair of bromines. Although, this geometry yielded triplets at 430 nm and 350 nm, several other triplets were predicted between the wavelengths.

One final question that needs to be addressed is how energy transfer occurs between the STE and Ce. It has been suggested [28] that a sequence of events leads to either prompt or delayed Ce emission. Prompt emission is suggested to be due

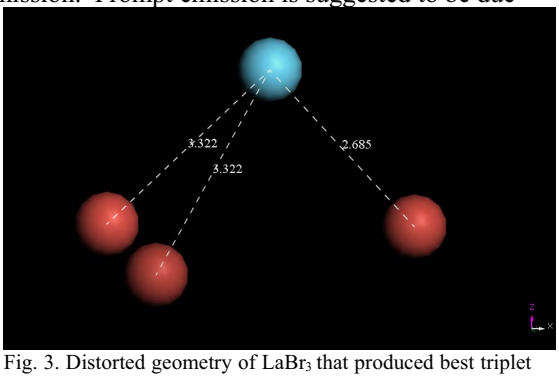

Fig. 3. Distorted geometry of $LaBr_3$ that produced best triplet wavelengths.

to direct excitation of Ce from the conduction band. The DoS calculation for 0.5% doped $LaBr_3$, shown in Fig. 4 indicate that the 4f and 5d levels of Ce are located at lower energies than the conduction band. Other Ce molecular orbitals are involved in the conduction band and may lead to this prompt emission. How the prompt emissions occurs is probably a direct excitation of Ce or direct creation of $CeBr^+$.

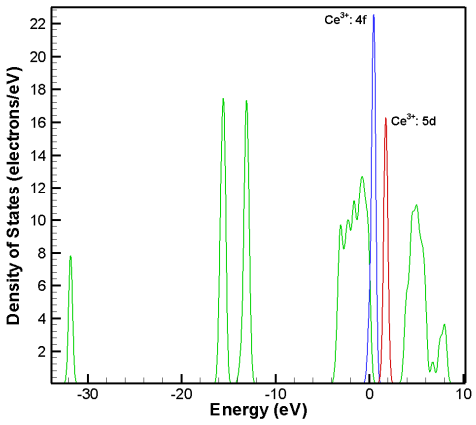

Fig. 4. DoS plot (CASTEP-DFT) for 0.5% Ce doped $LaBr_3$, green lines indicate La molecular orbitals and red and blue are Ce orbitals.

To further investigate the energy transfer process, the information shown in Table 3 was generated using DFT calculations, employing pseudopotentials for core electrons of all species, to understand the ground state energies of all the species that have been discussed. It is clear that both the Ce molecular total energy and energy of

the HOMO is lower in relation to respective La containing molecule. This implies that in the valence band, Ce is a low energy defect. Since DFT calculations are not accurate for excited state energies, it is not certain how the LUMO behaves. It is expected that the trend will be the same. Ce orbitals will be lower in energy that the corresponding La orbitals. In terms of the proposed energy transport model, Ce being a low energy trap will cause holes or V_k centers to migrate to these sites in the crystal [4]. In terms of the electron mobility, since $CeBr^+$ is also situated at lower energy than the corresponding $LaBr^+$, it will serve as a better electron trap.

TABLE 3
DFT Calculated total and HOMO energies expressed in Hartrees for $LaBr_3$, $LaCl_3$, $CeBr_3$, and $CeCl_3$ species.

Species	Total Energy (Ha)	HOMO Energy (Ha)
$LaBr_9$	-3105.0339	-0.27243
$CeBr_9$	-3114.9153	-0.26958
$LaBr_3$	-1073.1463	-0.20133
$CeBr_3$	-1083.055	-0.18610
$LaBr^+$	-395.649	-0.31129
$CeBr^+$	-405.322	-0.2995
$LaCl_9$	-4185.774	-0.30591
$CeCl_9$	-4195.582	-0.29989
$LaCl_3$	-1433.349	-0.22109
$CeCl_3$	-1443.359	-0.20470
$LaCl^+$	-515.542	-0.31592
$CeCl^+$	-525.427	-0.30688

IV. Discussion

The intent of this study was to better understand the molecular aspects of the scintillation mechanism in $LaBr_3$ and $LaCl_3$. This investigation has primarily focused on the mechanisms that involve formation of the STE. How the STE forms and how the STE transfers energy to the luminescent center (Ce) are considered using quantum mechanical approaches.

Based on prior work and bonding energies, the first stage in the process following absorption of a photon of energy greater than the band gap is formation of the electron and hole. Since the d and f orbital of La are the primary components of the conduction band, promotion of an electron into the conduction band puts the electron on the La. Electrons in the conduction band can be anywhere in the material, not just localized around the site of creation. At some time, the electron becomes trapped either by formation of $LaBr^+/LaCl^+$ or more likely $CeBr^+/CeCl^+$ from a molecular and binding energy perspective.

As a consequence of electron promotion to the conduction band, an electron deficiency or hole is created in the valence band. Since Br/Cl orbitals comprise the valence band, the hole resides on a Br or Cl. Given that the Br-Br distance in $LaBr_3$ is approximately 0.360 nm, Fig. 5 suggests that Br_2^- is stable and forms the molecular complex. A similar situation exists for Cl_2^-, however the stable bond length is shorter. Formation of the X_2^-(either Br or Cl) has two implications, it creates a stable species that has states that can not directly transfer to LaX_3 and be quenched. Second, Br_2^- is stable over a bond length region of approximately 0.250 to 0.430 nm. Br/Cl motion in the crystal will provide a mechanism for hole mobility.

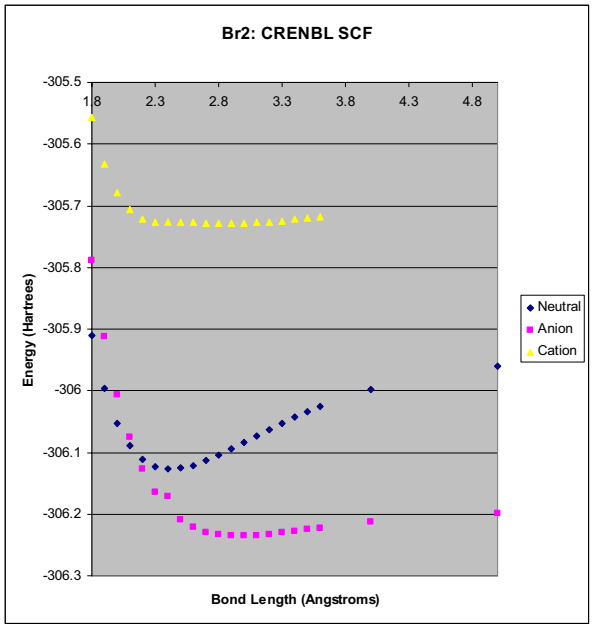

Fig 5. Calculated Br_2 bond energies as a function of bond length based on both DFT and HF-MP2 calculations. Energies are provided for molecule (diamond), anion (square) and cation (triangle).

The STE is created by the hole and electron combining to form LaX_3^*. This is a distorted complex having one La-X bond length considerably shorter than the equilibrium value for LaX_3. Two La-X bonds will be longer than the equilibrium value. The LaX_3^* forms by a combination of LaX^+ and X_2^- having one unpaired electron each. This formation creates a triplet and single excited state manifold and a singlet ground state. Based on experimental evidence, the STE is formed in a triplet state and this triple is suggested by modeling. This complex is loosely bonded due to the excess energy in the crystal and subsequent crystal vibrations or X movement can result in either stabilizing or destroying this species.

This creation and destruction of the LaX_3^* species seems to explain the temperature

dependence of the STE emission observed for $LaBr_3$ and $LaCl_3$. STE emission disappears above 100K for $LaBr_3$. The long stable bond length of Br_2^- and the Br spacing in the $LaBr_3$ lattice allows the $LaBr_3^*$ to migrate in the crystal via Br_2^- migration. In contrast, the bond length for stability of Cl_2^- is considerably shorter than Br and the Cl spacing in the lattice is approximately the same as $LaBr_3$. Much higher temperatures are required to create Cl motion of sufficient magnitude to decompose the STE and have Cl_2^- migration. Therefore, $LaCl_3$ STE emission persists to higher temperatures and this is experimentally observed.

Finally, this analysis suggests that there are three factors responsible for the scintillation /luminescence efficiency of $LaCl_3/LaBr_3$ when doped with Ce. The first is the involvement of La in the conduction band and $LaBr^+/CeBr^+$ serving as electron traps. Second is the mobility of the hole and STE in the form of X_2^- and LaX^+-X_2^-. The third is the lower energy of the Ce species serves as and energy minimum and sink that traps electrons and holes. This results in efficient energy transfer to the Ce bearing species. The isolation of the emitting Ce 5d states results in efficient conversion of ionizing radiation energy into Ce photons.

Thus, it is the finding of this study that the involvement of the host cation (in this case La) is what makes these $LaCl_3$ and $LaBr_3$ efficient hosts for Ce scintillators.

V. References

[1] E. V. D van Loef, P. Dorenbos, C. W. E. van Eijk, K. Krämer, and H. U. Güdel, "High-energy–resolution scintillator: Ce^{3+} activated $LaCl_3$," *Appl. Phys. Lett.* vol. 77 no. 10, 1467-1468, 2000.

[2] E. V. D. van Loef, P. Dorenbos, C. W. E. Van Eijk, K. Krämer, and H. U. Güdel, "High-energy-resolution scintillator: Ce^{3+} activated $LaBr_3$," *Appl. Phys. Lett.* vol. 79 no. 10, 1573-1575, 2000.

[3] E. V. D. van Loef, P. Dorenbos, C. W. E. Van Eijk, K. Krämer, and H. U. Güdel, "Influence of anion on the spectroscopy and scintillation mechanism in pure and Ce^{3+} doped K_2LaX_5 and LaX_3 (X=Cl, Br, I)," *Phys. Rev. B* vol. 68, 045108-1-9, 2003.

[4] P. Dorenbos, "Scintillation mechanism in Ce^{3+} halide scintillators," *phys. stat. sol. (a)* vol. 202 no. 2, 195-200, 2005.

[5] S. Zazubovich, "Physics of halide scintillators," *Rad. Measurement* vol. 33, 699-704, 2001.

[6] A. L. Shluger, J. L. Gavartin, M. A. Szymanski, A. M. Stoneham, "Atomistic modeling of radiation effects: Towards dynamics of exciton relaxation," *Nuc. Inst. Meth. Phys. Res. B* vol. 166-7, 1-12, 2000.

[7] S. Nakonechnyi, *et.al,* "Low-temperature excetonic, electron-hole and interstitial-vacancy processes in LiF single crystals," *J. Phys. Condens. Matter vol.* 18, 379-394, 2006.

[8] C. H. Leung, G. Brunet and K. S. Song, "Off-centre equilibrium configuration of the self-trapped exciton in alkali chlorides," *J. Phys. C:Solid State Phys* vol.18, 4459-4470, 1985.

[9] K. S. Song and R. T. Williams, "Temperature-dependent self-trapped exciton relaxation in alkali halides: molecular dynamics study," *phys. Stat. sol. (b)* vol. 243, no. 14, 3782-3794, 2006.

[10] J. L. Gavartin, P. V. Sushko and A. L. Shluger, "Modeling Charge self-trapping in wide-gap dielectrics: Localization problem in local density functionals," *Phys. Rev. B* vol. 67, 035108, 2003.

[11] A. L. Shluger, A. H. Harker, V. E. Puchin, N. Itoh and C. R. A. Catlow, "Simulation of defect processes: experiences with the self-trapped exciton," *Modelling Simul. Mater. Sci. Eng.* vol. 1, 673-692, 1993.

[12] M. Ratner, A. Ratner, T. Hryn'ova, "Excitonic energy transport in wide-band inorganic scintillators," *Nucl. Inst. Meth. Phys. Res. A* vol. 486, 463-470, 2002.

[13] M. Marsman, J. Andriessen and C. W. E. van Eijk, "Structure, optical absorption, and luminescence energy calculation for Ce^{3+} defects in $LiBaF_3$," *Phys. Rev. B.* vol. 51, no. 24, 16477, 2000.

[14] J. Andriessen, P. Dorenbos, and C. W. E. van Eijk, "*Ab initio* calculation of the contribution from anion dipole polarization and dynamic correlation to 4f-5d excitations of Ce^{3+} in ionic compounds," *Phys. Rev. B.* vol. 72, 045129, 2005.

[15] G. Lanza and C. Minichino, "Anharmonic, Temperature, and Matrix Effects on the Molecular Structure and Vibrational Frequencies of Lanthanide Trihalides LnX_3 (Ln-La, Lu; X=F, Cl)," *H. Phys. Chem. A* vol. 109, 2127-2138, 2005.

[16] S. J. Clark, M. D. Segall, C. J. Pickard, P. J. Hasnip, M. J. Probert, K. Refson, M. C. Payne, "First principles methods using CASTEP,' *Z. Kryst.* Vol. 220, nos. 5-6, 567-570, 2005.

[17] J. P. Perdew, A. Zunger, "Self-interaction correlation to density-functional approximations for many-electron systems," *Phys. Rev. B* vol 23, 5048-5079, 1981.

[18] R. Asahi, W. Nannstadt, and A. J. Freeman, "Optical properties and electronic structures of semiconductors with screened-exchange LDA," *Phys. Rev. B* vol. 59, no. 11, 7486-7492, 1999.

[19] C. Møller and M. S. Plesset, *Phys. Rev.* vol. 34, 618, 1934.

[20] E. Apra, *et.al*, "NWChem A Computational Chemistry Package for Parallel Computers, Version 4.6, 2006.

[21] Y. Shao, *et.al*, "Q-Chem, Version 3.0," Q-Chem, Inc. Pittsburgh, PA, 2006.

[22] D. Maurice and M. Head-Gordon, *J. Chem. Phys.* Vol. 103, 4160, 1995.

[23] R. B. Ross, S. Gayen, and W. C. Ermler, "Ab *initio* effective potentials with spin-orbit operators, V. Ce through Lu," *J. Chem. Phys.* vol. 100, 8145-8155, 1994.

[24] T. R. Cundari and W. J. Stevens, "Effective core potential methods for the lanthanides," *J. Phys. Chem.* vol. 98, 5555-5565, 1993.

[25] T. van Mourik and T. H Dunning, Jr., "Gaussian Basis Sets for Use in Correlated Molecular Calculations. VIII. Standard and Augmented Sextuple Zeta Correlation Consistent Basis Sets for Aluminum through Argon," *J. Quantum Chem.* Vol. 76, 205-221, 2000.

[26] B. Delley, "From molecules to solids with the $DMol^3$ approach," *J. Chem Phys.* vol. 113, 7756, 2000.

[27] B. Delley, "An all-electron numerical method for solving the local density functional for polyatomic molecules," *J. Chem. Phys.* vol. 92, 508-517, 1990.

[28] G. Bizarri and P. Dorenbos, unpublished results, 2007.

[29] S. Sato, "Optical Absorption and X-Ray Photoemission Spectra of Lanthanide and Cerium Halides," *J. Phys. Soc.* vol. 41, no. 3, 913-920, 1976.